



CrossMark
click for updates

Cite this: *RSC Adv.*, 2014, 4, 58204

Received 14th August 2014
Accepted 30th October 2014

DOI: 10.1039/c4ra08681c

www.rsc.org/advances

Liposomes containing mannose-6-phosphate-cholesteryl conjugates for lysosome-specific delivery†

E. Crucianelli,^a P. Bruni,^b A. Frontini,^c L. Massaccesi,^a M. Pisani,^b A. Smorlesi^c and G. Mobbili^{*a}

Lysosomes are promising targets for cancer and enzyme replacement therapy. In this area of interest we present a novel liposomal nano-carrier containing mannose 6-phosphate-cholesteryl conjugates and show its ability to reach the lysosomes by means of confocal and fluorescence microscopy measurements.

Lysosomes are the waste disposal system of the cell. Containing about 60 different hydrolytic enzymes, they are able to process all kinds of biomolecules internalized by the cell or obsolete cellular components.^{1,2} Lysosomal enzymes are acid hydrolases that are activated in the acidic environment of these organelles to ensure the normal function of the cell. Their deficiency leads to accumulation of substrates such as glycosphingolipids, mucopolysaccharides or glycogen in various tissues and generates over 50 different human lysosomal storage diseases (LSDs),³ for example lipid storage disorders, mucopolysaccharidoses, glycoprotein storage disorders and mucopolipidoses. Once synthesized, lysosomal hydrolases are provided of a mannose-6-phosphate (M6P) group through the action of a UDP-*N*-acetylglucosamine-1-phosphotransferase (GlcAc-1-phosphotransferase).^{4–8} The presence of the M6P tag makes lysosomal hydrolases recognizable by M6P receptors⁹ in the Golgi apparatus so that they can be transported to the lysosomal system *via* the secretory pathway through clathrin-coated vesicles. In mammalian cells two specific receptors of the *trans*-Golgi network recognize M6P-functionalized hydrolases: the cation-independent M6P receptor (CI-M6PR) and the cation-dependent M6P receptor (CD-M6PR), both type I transmembrane glycoproteins.^{10–12} CI-M6PR is especially localized in

the Golgi and endosomal compartments where acidity induces release of enzymes from M6P receptor which is recycled in the Golgi apparatus. A minor fraction of CI-M6PR is also present on the cell surface where it mediates the endocytosis and the transfer to lysosomes of secreted acid hydrolases, but also internalizes extracellular ligands,^{13–16} including M6P-containing proteins.^{17–21} CI-M6PR can therefore be considered an extremely interesting candidate that could be used to specifically target the transport of molecules into the lysosomes.

In the last years our research has been focused on the development of neutral liposomal delivery systems,^{22–24} artificial and biologically inert phospholipid vesicles that, by virtue of their amphiphilic nature, are capable of transporting both water-soluble and water-insoluble drugs inside the cells. Liposomes can increase the stability of the transported molecules by retarding their processing,²⁵ delaying drug clearance and, in general, improving the pharmacokinetic of the administered drug.

We propose here a new delivery system based on liposomes containing dioleoylphosphatidylcholine (DOPC) and M6P functionalized cholesterol. By virtue of its affinity for the CI-M6PR receptor, M6P group enables liposomes to carry bioactive molecules along the route leading to lysosomes. One of the principal therapeutic applications for M6P functionalized liposomes could be enzyme replacement therapy (ERT) for LSDs. ERT is usually performed by administering the enzyme to the patient through intravenous infusion.²⁶ An interesting approach²⁷ among the used ERT strategies is the administration of lysosomal hydrolases obtained through a protein expression system that provides the enzyme of higher levels of phosphorylated oligomannose residues correlating with increased binding to M6P receptors. However, this therapy presents some drawbacks such as the enormous cost and the limited life of enzymes in the circulation. The administration of lysosomal enzymes through the use of a M6P functionalized liposomes-based carrier system could improve the transport of the therapeutic contents into lysosomes through the CI-M6PR pathway while protecting the enzyme from a too rapid deactivation *in vivo*.

^aDi.S.V.A. Department, Università Politecnica delle Marche, Via Brecce Bianche, 60131 Ancona, Italy. E-mail: g.mobbili@univpm.it

^bSIMAU Department, Università Politecnica delle Marche, Via Brecce Bianche, 60131 Ancona, Italy

^cDepartment of Experimental and Clinical Medicine, Università Politecnica delle Marche, Via Tronto, 60126 Ancona, Italy

† Electronic supplementary information (ESI) available. See DOI: 10.1039/c4ra08681c

A further interesting application of lysosomotropic liposomes could be the induction of apoptotic pathways in cancer cells through the delivery of molecules, able to destabilize lysosomes and induce the release of lysosomal enzymes.^{28,29} Cell apoptosis can be caused by the activation of mitochondrial death pathway,³⁰ triggered by cathepsins,^{31–33} specific enzymes that are released from lysosomes following the permeabilization of lysosomal membranes (LMP). Relying on the fact that the majority of solid tumors, particularly breast cancers,³⁴ over-express CI-M6PR receptor, M6P functionalized liposomes could be used to transport and release into lysosomes specific molecules³⁵ that are able to induce LMP and consequently lead to the death of the cancer cell.

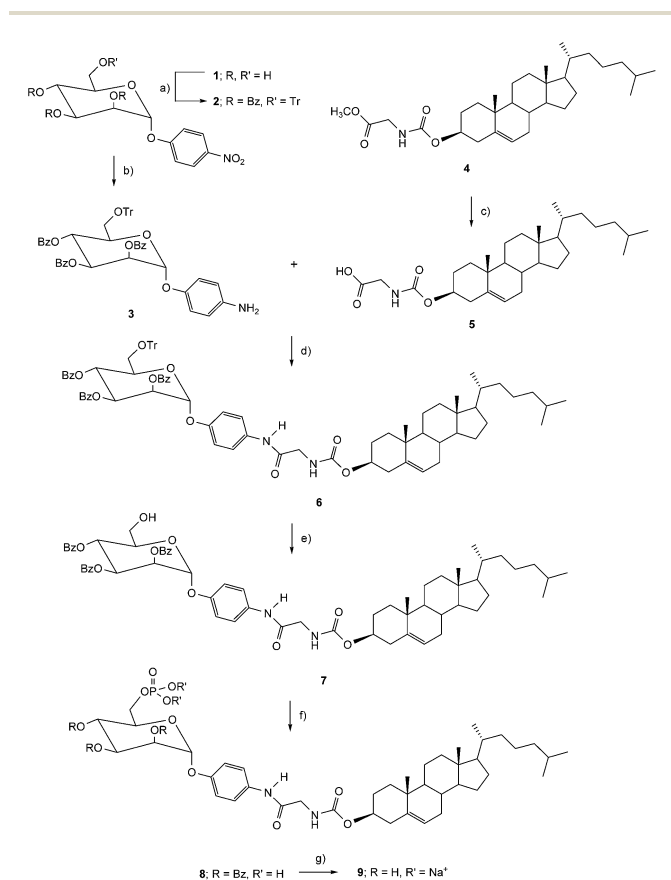
In the present study a M6P cholesteryl conjugate (Chol-M6P) was synthesized (Scheme 1) and employed with DOPC in the preparation of functionalized vesicles. To demonstrate the potential of our novel vector system, specifically designed to target lysosomes, we loaded the M6P functionalized liposomes with the model compound calcein and investigated the intracellular trafficking in a 3T3-NIH cell line using confocal and fluorescence microscopy technique.

The design of Chol-M6P is based on three requirements: it comprises (i) a lipophilic part acting as an anchor, enabling its

insertion into the lipid bilayer, (ii) a linker and (iii) at the opposite end of the spacer, a hydrophilic M6P group. With the aim to connect a M6P moiety to a steroid structure we chose a sufficiently rigid aryl-incorporated linker both to ensure an efficient exposure of the M6P function and to favour tight association of the liposome with the receptor by reducing the entropic cost of the process.³⁶ The apolar structure of the steroid provides stability to the drug delivery system because it is embedded into the lipid bilayer of liposomes spanning about half a layer. The tetracyclic apolar ring structure is compact and very rigid so that it increases the degree of order (cohesion and packing) in the liposome membrane and generally reduces the passive permeability to drugs encapsulated inside the lipidic vectors. The synthesis of Chol-M6P is drawn in Scheme 1 and described in detail in the ESI.† The 4-nitrophenyl- α -D-mannopyranoside **1** was selectively protected on the primary hydroxyl with a trityl group and on the secondary hydroxyl functionalities with benzoyl groups in one-pot reaction to give **2**. After purification by chromatography, the nitro group of compound **2** was converted by hydrogenation into an amino group to give **3**. Meanwhile, in order to synthesize the steroidal portion of the molecule, a cholesteryl chloroformate was added to a solution of the trifluoro acetate salt of a methyl ester glycine to give **4**. Subsequent hydrolysis of the ester furnished the corresponding acid **5**. Then compounds **3** and **5** were joined together *via* carbodiimide coupling to give **6**, which was selectively deprotected at C-6 with catalytic amount of *p*-toluene sulfonic acid. The resulting primary alcohol **7** was firstly converted into phosphate **8** and successively debenzoylated with NaOCH₃. Final treatment of compound **9** with Dowex cation exchange resin (Na⁺ form) afforded Chol-M6P as disodium salt. The structure of Chol-M6P was confirmed by NMR Spectroscopy and Mass Spectrometry (ESI†).

Liposomes were prepared by the “thin film hydration” method as reported in ESI.† Appropriate amounts of chloroform solutions of DOPC and cholesterol-M6P were mixed to obtain liposomes with different molar ratio (mol/mol) of DOPC/Chol-M6P (95 : 5, 90 : 10, 85 : 15, 80 : 20).

In order to verify the insertion of Chol-M6P inside the liposome bilayers we carried out ζ -potential measurements of all liposomal formulations by means of electrophoretic light scattering; in fact, the ζ -potential is correlated to the vesicle surface charge. The size of vesicles was also determined by dynamic light scattering. As reported in Table 1, the liposome mean diameter was in the range between 86 and 106 nm, with a low polydispersity index (PDI) between 0.18 and 0.25, which proved



Scheme 1 Reagents and conditions: (a) TrCl, DMAP, dry Py, 70 °C then BzCl, rt, on, 86%; (b) Pd/C 10%, H₂, dry CH₃OH, reflux, 73%; (c) NaOH 1 M, THF, 0 °C, 2 h then HCl 1 M, 95%; (d) DCC, DMAP, DCM, rt, 63%; (e) *p*-TsOH, CH₃OH, CHCl₃, 67%; (f) POCl₃, TEA, dry DCM, 0 °C, rt, 72%; (g) NaOCH₃, dry CH₃OH then Dowex Na cation exchange resin.

Table 1 Size and ζ -potential of DOPC/Chol-M6P liposomes

DOPC/Chol-M6P mol/mol	Size \pm SD (nm)	ζ -potential \pm SD (mV)
100 : 0	103.5 \pm 1.5	-13.2 \pm 1.6
95 : 5	86.5 \pm 0.6	-40.5 \pm 5.0
90 : 10	106.0 \pm 1.4	-57.1 \pm 7.2
85 : 15	101.1 \pm 1.4	-65.7 \pm 7.0
80 : 20	99.8 \pm 0.8	-72.1 \pm 8.8

that all dispersions used had very narrow vesicle size distribution. By increasing the concentration of the Chol-M6P in the DOPC liposomes, the negative ζ -potential values decreased, thus demonstrating the presence of negative M6P group on the liposome surface (Table 1).³⁷

The capability of M6P functionalized liposomes to be internalized by M6P-receptor expressing cells has been assessed through intracellular tracing experiments in NIH-3T3 cells.³⁸ For this purpose we decided to test the DOPC liposomes containing the highest percentage of Chol-M6P (as evidenced by their ζ -potential) in order to increase the cellular uptake.

We performed preliminary experiments by epi-fluorescence microscopy using DOPC/Chol-M6P liposomes encapsulating the reporter molecule calcein. In order to exclude non-specific endocytosis we used free calcein and calcein-loaded DOPC/cholesterol liposomes (80 : 20 mol/mol) as controls. We verified that, in the absence of M6P moiety, vesicles are not able to carry the fluorescent molecule into cells. Neither calcein alone is able to cross cell membrane and enter the cells (Fig. S1 in ESI†).

With the aim of better understanding the intracellular trafficking of DOPC/Chol-M6P liposomes we carried out confocal microscopy experiments. Calcein loaded Rhodamine-labeled DOPC/Chol-M6P liposomes were prepared and used in delivery experiments as described in ESI section.† Confocal microscopy analysis of treated cells revealed a clear localization of calcein (Fig. 1A) and liposomes (Fig. 1B) inside the cells at *peri*-nuclear position into small vesicles resembling lysosomes (Fig. 1C).

In order to establish the nature of the vesicles where calcein accumulated, we performed further assays on NIH-3T3 cells and used the lysosome-specific red fluorescent marker LysoTracker to label treated cells. Confocal microscopy analysis showed the presence of calcein (Fig. 2A) in the same vesicles that were labeled by LysoTracker (Fig. 2B) proving that calcein-loaded liposomes reached lysosomes according to our hypothesis. In the merged image, the yellow fluorescence showed the co-localization of calcein and lysosomal compartments (Fig. 2C).

Based on several trials, that we performed in the same experimental conditions, we have estimated a good efficiency for our system. For each performed assay, calcein loaded cells were counted in culture chambers. Calcein containing cells

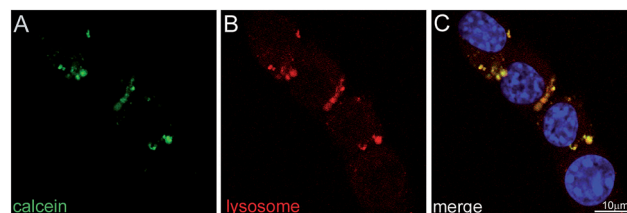


Fig. 2 Co-localization study performed by confocal microscopy. (A) Calcein visualized in green; (B) lysosomes labeled in red using LysoTracker; (C) by merging the previous two panels, calcein clearly resulted localized in lysosome structures (yellow).

(positive) appeared to be in equal proportion with negative ones but sometimes they appeared clustered in specific chambers and other time they showed a different pattern *i.e.* positive cells scattered among negative ones. Overall, we have estimated an average of 40–50% of cells that showed calcein internalization after treatment with functionalized liposomes.

Focusing more in detail on the confocal imaging of tracing experiment performed on NIH-3T3 cells (Fig. 1C inset) we observed that calcein and liposomes co-localize in among 80% of the vesicles (yellow). About 10% of the elements are instead represented only by calcein loaded vesicles (white arrow) and, the remaining 10% of the elements, are vesicles loaded with lipid alone (white arrowhead). We could then try to propose a model for the internalization pathway of our carrier liposomes by hypothesizing that, following the internalization of calcein-containing M6P-liposomes into the lysosomes (yellow vesicles), carrier lipids begin to be processed and degraded releasing the transported molecule in the lumen of the organelles (green vesicles) as suggested also by the fact that calcein itself is not internalized into cells.

At this stage of our work, liposomes containing Chol-M6P appears to be promising vector in selective targeting of lysosomes. Experiments *in vitro* and *in vivo* aimed at demonstrating the potential application of the system as pharmaceutical carrier in ERT and in anticancer therapy are being planned.

Acknowledgements

This work was supported by Genzyme Corporation.

Notes and references

- 1 R. Castino, M. Demoz and C. Isidoro, *J. Mol. Recognit.*, 2003, **16**, 337.
- 2 T. Bräulke and S. Bonifacino, *Biochim. Biophys. Acta*, 2009, **1793**, 605.
- 3 T. Lübke, P. Lobel and D. E. Sleat, *Biochim. Biophys. Acta*, 2009, **1793**, 625.
- 4 M. L. Reitman and S. Kornfeld, *J. Biol. Chem.*, 1981, **256**, 11977.
- 5 A. Waheed, A. Hasilik and K. von Figura, *J. Biol. Chem.*, 1981, **256**, 5717.
- 6 A. Varki and S. Kornfeld, *J. Biol. Chem.*, 1980, **255**, 10847.

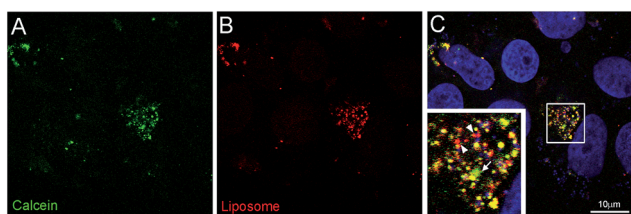


Fig. 1 Confocal microscopy analysis of NIH-3T3 treated cells. (A) Calcein visualized in green; (B) liposome visualized in red; (C) co-localization of calcein and liposome within individual cells (yellow). The complex are mainly found at *peri*-nuclear position and this is particularly evident in the inset of panel C, where nuclei were counterstained in blue using TO-PRO-3.

- 7 M. L. Reitman and S. Kornfeld, *J. Biol. Chem.*, 1981, **256**, 4275.
- 8 A. Waheed, A. Hasilik and K. von Figura, *J. Biol. Chem.*, 1982, **257**, 12322.
- 9 A. Kaplan, D. T. Achord and W. S. Sly, *Proc. Natl. Acad. Sci. U. S. A.*, 1977, **74**, 2026.
- 10 S. Kornfeld, *Annu. Rev. Biochem.*, 1992, **61**, 307.
- 11 R. Pohlmann, M. W. Boeker and K. von Figura, *J. Biol. Chem.*, 1995, **270**, 27311.
- 12 D. E. Sleat and P. Lobel, *J. Biol. Chem.*, 1997, **272**, 731.
- 13 X. Ni, M. Canuel and C. R. Morales, *Histol. Histopathol.*, 2006, **21**, 899.
- 14 A. Nykjaer, E. I. Christensen, H. Vorum, H. Hager, C. M. Petersen, H. Roigaard, H. Y. Min, F. Vilhardt, L. B. Moller, S. Kornfeld and J. Gliemann, *J. Cell Biol.*, 1998, **141**, 815.
- 15 Y. Oka, L. M. Rozek and M. P. Czech, *J. Biol. Chem.*, 1985, **260**, 9435.
- 16 J. X. Kang, Y. Li and A. Leaf, *Proc. Natl. Acad. Sci. U. S. A.*, 1997, **94**, 13671.
- 17 S. Kornfeld and I. Mellman, *Annu. Rev. Cell Biol.*, 1989, **5**, 483.
- 18 M. E. Wolk and J. A. Trapani, *Microbes Infect.*, 2004, **6**, 752.
- 19 C. R. Brunetti, K. S. Dingwell, C. Wale, F. L. Graham and D. C. Johnson, *J. Virol.*, 1998, **72**, 3330.
- 20 F. Blanchard, S. Raheer, L. Duplomb, P. Vusio, V. Pitard, J. L. Taupin, J. F. Moreau, B. Hoflack, S. Minvielle, Y. Jacques and A. J. Godard, *Biol. Chem.*, 1998, **273**, 20886.
- 21 D. Metcalf, *Stem Cells*, 2003, **21**, 5.
- 22 P. Bruni, O. Francescangeli, M. Marini, G. Mobbili, M. Pisani and A. Smorlesi, *Mini-Rev. Org. Chem.*, 2011, **8**, 38.
- 23 M. Pisani, G. Mobbili, I. F. Placentino, A. Smorlesi and P. Bruni, *J. Phys. Chem. B*, 2011, **115**(34), 10198.
- 24 G. Angelini, M. Pisani, G. Mobbili, M. Marini and C. Gasbarri, *Biochim. Biophys. Acta*, 2013, **1828**(11), 2506.
- 25 T. M. Allen, M. S. Newman, M. C. Woodle, E. Mayhew and P. S. Uster, *Int. J. Cancer*, 1995, **62**, 199.
- 26 G. A. Grabowski and R. J. Hopkin, *Lancet*, 2003, **372**, 1263.
- 27 K. Lee, X. Jin, K. Zhang, L. Copertino, L. Andrews, J. Baker-Malcolm, L. Geagan, H. Qiu, K. Seiger, D. Barngrover, J. M. McPherson and T. Edmunds, *Glycobiology*, 2003, **13**(4), 305.
- 28 T. Kirkegaard and M. Jäättelä, *Biochim. Biophys. Acta*, 2009, **1793**, 746.
- 29 G. Kroemer and M. Jäättelä, *Nat. Rev. Cancer*, 2005, **5**, 886.
- 30 P. Boya, K. Andreau, D. Poncet, N. Zamzami, J.-L. Perfettini, D. Metivier, D. M. Ojcius, M. Jäättelä and G. Kroemer, *J. Exp. Med.*, 2003, **197**(10), 1323.
- 31 K. Roberg, K. Kagedal and K. Ollinger, *Am. J. Pathol.*, 2002, **161**, 89.
- 32 B. Turk, I. Dolenc, V. Turk and J. G. Bieth, *Biochemistry*, 1993, **32**, 375.
- 33 B. Turk, V. Stoka, J. Rozman-Pungerčar, T. Cirman, G. Droga-Mazovec, K. Orešič and V. Turk, *Biol. Chem.*, 2002, **383**, 1035.
- 34 G. Kroemer and M. Jäättelä, *Nat. Rev. Cancer*, 2005, **97**(5), 886.
- 35 A. Koshkaryev, A. Piroyan and V. P. Torchilin, *Cancer Biol. Ther.*, 2012, **13**(1), 50.
- 36 M. Mammen, E. I. Shakhnovich, J. M. Deutch and G. M. Whitesides, *J. Org. Chem.*, 1998, **63**, 3821.
- 37 C. Sou and E. Tsuchida, *Biochim. Biophys. Acta*, 2008, **1778**, 1035.
- 38 K. von Figura, A. Waheed and A. Hasilik, *J. Biosci.*, 1983, **5**, 19.